

NASA Technical Memorandum 100996

NASA-TM-100996 19880014378

---

# Flight Testing a V/STOL Aircraft to Identify a Full-Envelope Aerodynamic Model

---

B. David McNally and Ralph E. Bach, Jr.

---

FOR REFERENCE

NOT TO BE TAKEN FROM THIS ROOM

May 1988

LIBRARY COPY

JUN 27 1988

LANGLEY RESEARCH CENTER  
LIBRARY NASA  
HAMPTON, VIRGINIA

  
National Aeronautics and  
Space Administration



---

# Flight Testing a V/STOL Aircraft to Identify a Full-Envelope Aerodynamic Model

---

B. David McNally  
Ralph E. Bach, Jr., Ames Research Center, Moffett Field, California

May 1988



National Aeronautics and  
Space Administration

**Ames Research Center**  
Moffett Field, California 94035

*N88-23762#*



FLIGHT TESTING A V/STOL AIRCRAFT TO IDENTIFY A  
FULL-ENVELOPE AERODYNAMIC MODEL

B. David McNally\* and Ralph E. Bach, Jr.†  
NASA Ames Research Center, Moffett Field, California

Abstract

Flight-test techniques are being used to generate a data base for identification of a full-envelope aerodynamic model of a V/STOL fighter aircraft, the YAV-8B Harrier. The flight envelope to be modeled includes hover, transition to conventional flight and back to hover, STOL operation, and normal cruise. Standard V/STOL procedures such as vertical takeoff and landings, and short takeoff and landings are used to gather data in the powered-lift flight regime. Long (3-5-min) maneuvers which include a variety of input types are used to obtain large-amplitude control and response excitations. The aircraft is under continuous radar tracking; a laser tracker is used for V/STOL operations near the ground. Tracking data are used with state-estimation techniques to check data consistency and to derive unmeasured variables, for example, angular accelerations. A propulsion model of the YAV-8B's engine and reaction control system is used to isolate aerodynamic forces and moments for model identification. Representative V/STOL flight data are presented. The processing of a typical short-takeoff and slow-landing maneuver is illustrated.

Introduction

Ames Research Center is conducting a flight research program on guidance, control, and display concepts for vertical/short takeoff and landing (V/STOL) aircraft. The goal of the program is to develop integrated propulsion and flight-control technology which would allow advanced short-takeoff and vertical-landing aircraft to operate in very low visibility conditions. The purpose of this paper is to describe the flight-test techniques and major elements of postflight data processing that are being used to build a data base to identify a full-envelope aerodynamic model of the NASA V/STOL Research Aircraft (VSRA). The model will be used to update and improve an existing VSRA simulation, which will aid in design of advanced guidance, control, and display systems for the aircraft.<sup>1</sup>

The flight-test techniques described in this paper were developed for the purpose of identifying a full-envelope aerodynamic model using regression methods<sup>2-6</sup> for parameter identification and state-estimation methods<sup>6-11</sup> for data reconstruction. The nonlinear model formulation requires large

variations in control and response variables during flight testing. The VSRA data base consists of a series of 3-5-min flight-test maneuvers that together cover the complete flight envelope and include time-histories of all relevant aircraft control and response variables. Concatenated segments from several of these maneuvers will be used to identify the unknown parameters in each model equation. Flight-test planning and the important aspects of postflight processing necessary to acquire the data base are covered. The modeling of VSRA aerodynamics will be covered in a later report.

The basis of a full-envelope aerodynamic model is a set of functions of control and response variables that when multiplied by the identified model parameters, represent aerodynamic force and moment coefficients. This set of functions is nonlinear in the control and response variables, such as nozzle angle, thrust setting, angles of attack and sideslip, and Mach number, but is linear in the parameters to be identified.<sup>5,12-14</sup> Regression methods are well suited for identifying a nonlinear model that is linearly parameterized. Further, regression methods are computationally simple and are therefore well suited to processing large amounts of data. The straightforward numerical requirements of the regression method allow the analyst to concentrate on structuring an accurate and physically meaningful model. Good results with regression methods, however, are highly dependent on the quality of the data records. State-estimation methods are used before modeling to check instrument accuracy and to provide estimates of unmeasured or poorly measured variables.

Application of state estimation to aircraft flight data is possible because the measurements of an aircraft's motion along its flightpath are related by well-known kinematic relationships. As Breeman et al.<sup>6</sup> point out, state estimation makes use of the redundancy present in inertial and air data measurements in order to obtain the best estimate of aircraft state variables during a maneuver. The first application of state estimation to postflight data analysis can probably be attributed to Otto Gerlach in the 1960s at the Delft Technological University, the Netherlands. This early contribution, called "flightpath reconstruction," was primarily concerned with accurate determination of angle of attack, pitch angle, and vehicle velocity during dynamic maneuvers.<sup>15</sup> These "states" were obtained by integrating functions of measurements from the pitch-rate gyro and normal and longitudinal accelerometers. The resulting "smoothed" time-histories were then used as a basis for subsequent parameter identification studies. In this country, Wingrove at NASA was an early advocate of

\*Aerospace Engineer, Member AIAA.

†Aerospace Engineer, Member AIAA, IEEE.

This paper is declared a work of the U.S. Government and therefore is in the public domain.

Presented at the AIAA 4th Flight Test Conference  
San Diego, California, May 18-20, 1988. <sup>1</sup>

state estimation for flightpath reconstruction.<sup>16</sup> Over the past few years, work in this field has been evolving toward the use of more complete models, the development of more sophisticated algorithms, and the treatment of more difficult applications.<sup>7</sup> State-estimation methods are now used by many flight-test groups.<sup>8-11</sup> Application of state estimation to flight data produces a consistent set of smoothed state time-histories for aerodynamic model identification.

The next section describes the test aircraft, the data acquisition system, and the flight-test facility. Flight-test planning and a description of the test maneuvers used to cover the flight envelope are then presented, with the trim points and specific maneuvers flown at each point given in tabular format. Preliminary processing, state estimation, and the calculation of aerodynamic forces and moments are then discussed and, finally, time-histories of representative flight-test maneuvers are presented. A particular V/STOL maneuver is used to illustrate the processing necessary to compute the body-axis aerodynamic forces and moments required for aerodynamic model identification.

#### Test Aircraft and Flight Data Acquisition

The VSRA (Fig. 1) is a YAV-8B, a prototype of the currently operational subsonic, vectored-thrust, AV-8B Harrier fighter aircraft; its engine nozzles can be rotated from 0° for forward flight to somewhat greater than 90° for hover and vertical flight. A reaction control system (RCS), in which compressor air is piped to the extremities of the aircraft, provides attitude control in hover and low-speed flight.

The VSRA measurement system is equipped with a 10-bit digital data-acquisition and telemetry (TM) system. A pulse-code modulation (PCM) format is used to encode 156 main-frame channels sampled at 120 Hz, and 160 sub-frame channels sampled at 30 Hz. Before encoding, each analog channel is passed through a third-order Butterworth anti-aliasing filter with its cutoff frequency set at one-fifth of the channel sampling rate. After encoding, all flight data are transmitted to a ground station where they are recorded. A partial list of on-board measurements, those necessary for aerodynamic model identification, is given in Table 1.

Flight tests of the VSRA were performed at the NASA facility located at Crows Landing, California. The facility control room, which has a clear view of the runway and hover pad, is equipped with five eight-channel strip-chart recorders and three color monitors for real-time display of the TM data. Two on-site radar systems are available to provide continuous tracking of the test aircraft's position. A laser tracker, bore sighted on one of the radar antennas, was used during V/STOL operation in order to obtain a more accurate

measurement of altitude above the ground (1.0 ft range error; 0.2 mrad azimuth and elevation error at 30,000 ft range). During flight test, TM data from the VSRA on-board system are downlinked and merged, at the facility, with range, bearing, and elevation data from the tracking systems; they are then recorded.

### Flight-Test Planning and Maneuver Design

#### Flight-Test Planning

The VSRA aerodynamic model must represent the three body forces and three moments over a flight envelope that includes hover, transition to forward flight and back to hover, as well as STOL operation and normal cruise. Large-amplitude control inputs are appropriate since the model being identified has a full-envelope formulation composed of nonlinear functions of aircraft control and response variables. If the objective is to use flight data to identify a linear perturbation model about some trim point then one must be careful not to let the aircraft's control and response variables exceed the linear bounds during flight test. However, if the objective is to identify a nonlinear model, as it is in this study, control and response variables should have large-amplitude variations to cover the flight envelope. In most cases the trim point is defined by one of the variables (e.g., Mach number, angle of attack) in the nonlinear model equation. Therefore, any deviations from the trim conditions during a flight-test maneuver are accounted for during model identification.

This relaxed trim requirement led to the idea of using "integrated" maneuvers that include a variety of consecutively executed control inputs. Maneuvers such as these make efficient use of flight time, since the aircraft does not have to be retrimmed between control inputs. Furthermore, they reduce the complexity of the bookkeeping required during postflight data processing, since the data base contains fewer (but longer) maneuvers. Meaningful and accurate model parameter estimates require that the maneuvers that make up the data base reflect independent variation of the control and response variables that define the aerodynamic model. Flight-test maneuvers and the matrix of nominal trim conditions were designed to meet this requirement.

Flight testing for VSRA aerodynamic model identification began in September 1987 and continued for 3 months. A total of 76 maneuvers were performed in 13 flights (each flight is marked by a refueling). The VSRA was configured with gun pods on and wing pylons off. Most maneuvers were performed with the stability augmentation system (SAS) off to obtain the natural open-loop dynamic response of the aircraft to the control inputs. As Maine and Iliff point out, automatic feedback systems (e.g., SAS) may make it difficult to excite the dynamics of the system, and may create linear dependencies between model terms.<sup>17</sup> Flight-test

cards, such as the one shown in Fig. 2, which gave the control inputs at their relative position on a ground track, were used to define most of the maneuvers described in this section. The flight-test cards fit on the pilot's knee board.

#### V/STOL Maneuvers

One characteristic that sets the VSRA apart from conventional aircraft is that it exhibits significant thrust-induced aerodynamic effects when the nozzles are not in the full-aft position. These effects are largest during transition from hover to conventional flight (and back to hover), and during low-speed flight. Standard V/STOL procedures, such as vertical takeoff and transition to conventional flight, transition to hover and vertical landing, short takeoff and transition to conventional flight, and slow landings were used to provide data for identification of thrust-induced aerodynamics.

A short-takeoff and slow-landing (STO-SL) maneuver, is outlined on the flight-test card shown in Fig. 2. In this maneuver, the ground roll begins with nozzles at 10°. At nozzle rotation speed  $V_r$ , the nozzles are rotated to an angle  $\theta_r$  (in the example for this paper,  $V_r = 50$  KIAS and  $\theta_r = 55^\circ$ ). Shortly after liftoff, the nozzles are rotated to the full aft position. For the slow-landing portion, nozzles are rotated to 40° just before the final turn, and during the final approach are further rotated to 60°. Three STO-SL maneuvers (outlined in Fig. 2) were performed during flight testing.

A vertical-takeoff and vertical-landing (VTO-VL) maneuver, similar to the STO-SL maneuver shown in Fig. 2, also provides data in the powered-lift flight regime. Just before takeoff, the nozzles are set to 81° (hover stop). Full throttle is added and the aircraft lifts vertically off the ground. When the aircraft is no longer in ground effect (above about 50 ft), the nozzles are slowly rotated aft for transition to conventional forward flight. As the aircraft gains aerodynamic lift during the transition, thrust is reduced as required. This maneuver has downwind and base legs similar to those of the STO-SL maneuver. At about 1 n. mi. from the touchdown point during the final approach, the nozzles are rotated from 40° to 81° and thrust is then used to control rate of descent and angle of attack. At an airspeed of about 50 knots a pitch flare is used to further reduce airspeed and bring the aircraft to a steady hover at about 50-100 ft above the touchdown point. Before landing, the pilot initiates a series of pitch, roll, and yaw doublets to measure reaction-control-system effectiveness in hover. Two VTO-VL maneuvers were performed.

V/STOL procedures were also performed out of ground effect (OGE) in order to aid separation of ground-effect aerodynamics. During an OGE slow-landing approach, the aircraft transitions to up-and-away flight at the airspeed at which it

would have touched down during a normal slow landing. During OGE procedures, the aircraft never descends below 100 ft above ground level.

#### Jet Velocity Ratio-Angle of Attack Maneuver

In the transition region, the aerodynamic model is strongly dependent on angle of attack (AOA) and equivalent jet velocity ratio (VEJ).<sup>1</sup> VEJ is inversely proportional to thrust-induced aerodynamics, and is defined as the square root of the ratio of free-stream dynamic pressure to engine jet exhaust dynamic pressure:

$$VEJ = (q_0/q_{jet})^{1/2} \quad (1)$$

The "VEJ-AOA" maneuver outlined in Fig. 3 was developed to generate large independent variation of VEJ and AOA at various nozzle and flap settings. The nominal trim points, listed in Table 2, are defined by nozzle, flap, and angle of attack. Most of these maneuvers were performed with "STOL Flap" mode engaged so flaps were scheduled as a function of nozzle angle.<sup>10</sup> It should be noted that the flaps cannot be selected independently of the nozzles beyond 25° flap deflection.

STOL flaps are normally engaged during V/STOL operation. During the first segment of the maneuver, thrust is slowly added, while using pitch control to hold angle of attack nearly constant, until the maximum continuous thrust setting is reached. Then thrust is slowly reduced, again holding angle of attack, until the pitch-authority limit is reached. Since  $q_{jet}$  is proportional to thrust, this segment effects a large change in  $q_{jet}$  at a nearly constant angle of attack. At the end of the first segment the aircraft is at a high altitude and low airspeed. During the second segment the pilot reduces thrust to idle and pushes the aircraft over into a dive to 400 knots. If flaps are extended, they are retracted to 25° so as not to violate airspeed-flap deflection limits; nozzles remain fixed at the trim setting. This segment effects a large change in  $q_0$  at a low value of  $q_{jet}$ . At the end of the maneuver the nominal trim condition and heading are restored. Seventeen VEJ-AOA maneuvers were performed.

#### Longitudinal Maneuver

The longitudinal maneuver (Fig. 4) excites large changes in longitudinal variables (angle of attack and pitch rate) from several nominal trim points. The trim points, listed in Table 3, are defined by either Mach number or angle of attack at constant nozzle angle and flap deflection. Thrust is held constant while the stabilator is varied to obtain changes in angle of attack and pitch rate. During the trim segment the aircraft is held in trim for 10 or 15 sec.

The first control inputs are pulses designed to generate maximum positive and negative pitch rates. The next input is a frequency sweep; the pilot moves the stick fore and aft in a sinusoidal

motion of smoothly increasing frequency. The starting frequency is well below the aircraft's short-period frequency and the ending frequency is high enough so that pitch response is significantly attenuated. The magnitude of the input is large enough to obtain the desired dynamic excitation. Following the 180° turn, the pilot regains the trim Mach number by diving to gain airspeed. Then the "AOA ladder" is used to obtain large variations in angle of attack by ramping AOA to a maximum value in an oscillatory fashion (see Fig. 5). During the AOA ladder the aircraft gains altitude and loses airspeed, and the pilot again regains the trim Mach number by diving. Next the "wind-up" turn results in a steady ramp in angle of attack. The technique is to roll the aircraft to an appropriate angle (about 40° for the maneuver shown in Fig. 5) and then slowly pull back on the stick until the angle of attack or normal acceleration limit, whichever comes first, is reached. In order to hold Mach number constant the aircraft descends during the wind-up turn. To end the maneuver, thrust is added to return to the nominal trim point. It should be emphasized that a considerable variation in Mach number may be experienced during the maneuver. Twenty-six of these longitudinal maneuvers were performed.

#### Lateral Maneuver

The lateral maneuver (Fig. 6) was designed to excite large changes in lateral axis variables (angle of sideslip, yaw rate, and roll rate). The trim points for the lateral maneuvers are also listed in Table 3. The trim segment is followed by wings-level sideslips to maximum left and right sideslip angle. The next input excites the Dutch roll mode using a rudder doublet immediately followed by an aileron doublet. After the turn, the pilot regains the trim Mach number using altitude, as with the longitudinal maneuver. A wings-level rudder frequency sweep and a rudder-fixed aileron frequency sweep provide additional lateral-axis excitation. The pilot uses aileron control to hold the wings-level condition during the sideslip and the rudder sweep portions of the maneuver. An initial roll angle of 40° was chosen for the aileron sweep. Thrust is added at the end of the maneuver to return to the nominal trim point. Thirteen of these lateral maneuvers were performed.

#### Preliminary Processing

Following real-time acquisition of data during flight test, each recorded maneuver, with instrument calibrations added, is converted to engineering units and made available to researchers as a raw flight-data file. An interactive program called PRODAT (PROcess DATa) is used to read the raw flight-data file, identify wild points, and filter data records. Data are then stored in a "processed" file of selected channels at a submultiple of the main-frame sample rate. PRODAT runs on a VAX-8650. Processing begins by removing wild points from the records. Several methods are

available, but one effective (and time-consuming) method is to pass each record through a "moving window." Points that fall outside the window are considered wild, and are tagged but not removed.

When all wild points in a record have been tagged, the record is passed through a zero phase-shift low-pass digital filter<sup>19</sup> to obtain a time-history free of wild points. The filter provides a least-squares fit to the "good" points in the data record. The algorithm consists of backward-filter, forward-smoother passes that yield a frequency response equivalent to cascaded second-order Butterworth filters with equal but opposite phase shift characteristics. After filtering, the data rate can be reduced to a submultiple of the main-frame sampling frequency. The filter cutoff frequency is set at one-half the final data rate desired. That data rate was chosen to be 20 Hz for all VSRA maneuvers.

Each channel processed from a maneuver raw-data file is stored in a processed flight-data file set up for that maneuver. An interactive program called DSPDAT (DiSPlay DATa), also running on the VAX-8650, is used to select processed data channels for plotting in either x-y or strip-chart format. An x-y cross-plot, for example, might display equivalent jet velocity ratio or Mach number plotted against angle of attack. Such plots offer a convenient way to evaluate how well the flight envelope has been covered during a maneuver. It is unlikely that a single maneuver will provide enough variation in aircraft control and response variables to identify all model terms; the analyst may also use DSPDAT to create or access a "map" file, which contains addresses of time segments selected from several processed maneuvers. This file can later be used to concatenate the selected segments to create a long record suitable for model identification.

#### State Estimation

The next step in the processing of each maneuver is to apply SMACK<sup>19-21</sup> (SMoothing for AirCRAFT Kinematics), a state-estimation program developed at Ames Research Center, to check data consistency and derive unmeasured variables. SMACK runs on a Cray-XMP computer. State estimation in this paper refers to a process that solves a state model,

$$\dot{x} = f(x,w), \quad x(t_0) = x_0 \quad (2)$$

such that  $h(x)$  in the measurement model

$$z = h(x) + v \quad (3)$$

suitably matches the data record over a time interval  $(t_0, t_f)$ , usually in a least-squares error sense.<sup>7,22</sup> In Eq. (2),  $x$  is the state vector and  $w$  is a vector that represents unknown forcing functions (derivatives of unmeasured variables, e.g., angular accelerations). For aircraft problems, the state and measurement models together



represent the kinematics of a rigid body for describing motion over a flat, nonrotating Earth. In the SMACK formulation, the state model consists of Euler angles and position variables and their derivatives. When flightpath winds are to be identified, the state model is augmented by wind velocities and accelerations. The measurement model generates time-histories which include on-board variables such as Euler angles, angular rates, and linear accelerations, as well as tracking variables such as range, bearing, and elevation (see Table 1). Any bias or scale-factor errors associated with the state or measurement models are appended to the state vector and treated as constant but unknown parameters. Static pressure and airflow measurements are corrected, based on recent VSRA flight tests, before they are input to the state estimation program.<sup>23</sup>

Solution of the state-estimation problem consists of determining the  $x$  and  $w(t)$  that minimize the squared-error performance measure,

$$J = (x_0 - \bar{x}_0)^T P_0^{-1} (x_0 - \bar{x}_0) / 2 - \int_{t_0}^{t_f} \{ [z - h(x)]^T R^{-1} [z - h(x)] + w^T Q^{-1} w \} dt / 2 \quad (4)$$

subject to the dynamic constraint of Eq. (2). In Eq. (4),  $\bar{x}_0$  is an a priori estimate of  $x_0$ ;  $P_0$ ,  $Q$ , and  $R$  are weighting matrices. Note that the first term of Eq. (4) serves as a "penalty" function and tends to bias the estimate of  $x$  toward its a priori value.

Long (3-5 min) maneuvers with large variations in the dynamic variables are well suited to analysis using state-estimation techniques. Each maneuver covers a nearly oval ground track within 5 min while under continuous radar track. The oval course allows the aircraft to stay at close range (within 10 miles for most cases) in order to minimize radar inaccuracies. Large heading changes (180° to 360°) facilitate identification of beta vane scale factors and ambient winds. The turns in the oval track provide the state-estimation algorithm with adequate variation in roll and heading during longitudinal axis maneuvers.

#### Force and Moment Calculations

The aerodynamic forces and moments acting on the VSRA during flight test are determined as the difference between the total forces and moments, and engine forces and moments. Here the term "engine" includes the reaction control system, as well as the main nozzles. The engine forces and moments are calculated by a program (VAX-8650) called ENCAL (ENgine CALculations). ENCAL uses a nominal propulsion model of the VSRA's Pegasus engine (YF402-RR-404) (Ref. 18). Fan dynamics are not included in this version, since fan speed is

measured in flight. It should be noted that the propulsion model provides only thrust forces and moments. Any thrust-induced aerodynamic effects are to be included in the VSRA aerodynamic model.

Inputs to the ENCAL routine include all the air-data, reaction control, engine, and weight measurements listed in Table 1. Outputs to the processed flight-data file are the three body-axis components of engine forces and moments. ENCAL also calculates aircraft weight and inertias, and the variation in center-of-gravity (c.g.) location (inertia and c.g. variations are based on manufacturers estimates as a function of fuel, water, landing gear, and stores).<sup>18</sup> These variables are added to the processed-data file. It should be emphasized that the aerodynamic model to be identified from flight data can only be as accurate as the engine, weight and inertia, and c.g. variation models. A newly instrumented Pegasus engine will be installed on the VSRA in the spring of 1988 (Ref. 24). Plans are being developed to validate the engine and inertia models based on data from the next set of flight tests.

Total VSRA force and moment time-histories are obtained from the SMACK-derived estimates of accelerations and angular rates, and from ENCAL-derived estimates of weight and inertias. The body-axis forces are given by

$$F_x = ma_x ; \quad F_y = ma_y ; \quad F_z = ma_z \quad (5)$$

where  $m$  is vehicle mass, and  $a_x$ ,  $a_y$ , and  $a_z$  are the body linear accelerations. The moments are calculated from

$$\left. \begin{aligned} T_l &= I_{xx} a_l - I_{zx} (a_n + pq) - (I_{yy} - I_{zz}) qr \\ T_m &= I_{yy} a_m - I_{zx} (r^2 - p^2) - (I_{zz} - I_{xx}) pr \\ T_n &= I_{zz} a_n - I_{zx} (a_l - qr) - (I_{xx} - I_{yy}) pq \end{aligned} \right\} \quad (6)$$

were  $I_{xx}$ ,  $I_{yy}$ ,  $I_{zz}$ , and  $I_{zx}$  are vehicle moments of inertia;  $a_l$ ,  $a_m$ , and  $a_n$  are the body angular accelerations; and  $p$ ,  $q$ , and  $r$  are the body angular rates.

#### Example Maneuvers

Figure 5 shows the variation in stabilator angle, pitch rate, and angle of attack during a longitudinal maneuver with nozzles at 60° and flaps at 60°. The trim airspeed and altitude for this maneuver were 85 knots (indicated) and 10,000 ft, respectively. The trim angle of attack was 10°. This maneuver contains large-amplitude inputs which result in large variations in angle of attack and pitch rate. Note the correlation with the maneuver description in Fig. 4.

## Concluding Remarks

Figure 7 shows the variation in engine rpm, true airspeed, and angle of attack during the first segment of a VEJ-AOA maneuver with nozzles at 60° and flaps at 60°. The trim angle of attack is about 9°. A cross-plot showing jet velocity ratio versus angle of attack for the time segment of Fig. 7 is shown in Fig. 8. The cross-plot shows relatively large variation in VEJ (0.13 to 0.8) over a 3° angle-of-attack range (7.7° to 10.7°). During normal flight operations the VSRA experiences jet velocity ratios ranging from 0 to about 1.2.

Figure 9 shows the variation in nozzle angle, flap setting, rpm, and control-surface positions during a STO-SL maneuver. Notice that the ailerons are set to a 15° down neutral position (i.e., drooped) during takeoff and landing.<sup>18</sup> In this maneuver, which contains abrupt changes in nozzle and flap angles, the aircraft transitions to normal flight after takeoff, performs a go-around, and then transitions back to a STOL configuration for a slow landing. This maneuver will serve to illustrate the results of the state-estimation procedure and the force and moment calculations.

The aircraft dynamic response to the control inputs is analyzed by the state-estimation procedure, which determines integrator initial conditions, selected instrument bias and scale-factor errors, and forcing-function time-histories that provide the best fits to the radar track and on-board measurements shown in Table 1. The body angular accelerations, true airspeed, and flight-path winds are estimated. During a preliminary solution, a large error was noticed in the fit of longitudinal acceleration during the takeoff portion of the maneuver. The longitudinal accelerometer had saturated at 0.6 g's, and its output in that interval had to be "blanked." Fortunately, the good tracking data provided the redundancy necessary to yield an estimate of longitudinal acceleration during the interval. Results of the SMACK analysis required for calculating forces and moments are shown in Fig. 10.

The large activity in the angular acceleration estimates in Fig. 10b is related to the reduced damping of the aircraft with the SAS turned off. This requires that the pilot provide more compensation to stabilize the aircraft. The control-surface movements in these test data are well correlated with the angular rate oscillations. A similar maneuver flown with the SAS on shows significantly smaller control-surface movements and angular rate oscillations.

In a final step, the aerodynamic forces and moments are calculated as the difference of total and engine forces and moments as outlined in the previous section. These are the time-histories that must be adequately represented by the VSRA aerodynamic model. Results of the ENCAL calculations for the maneuver are shown in Fig. 11; corresponding aerodynamic variables are shown in Fig. 12.

The flight-test techniques used to generate a data base suitable for identifying an aerodynamic model of a V/STOL aircraft using a regression procedure have been described. Test maneuvers were designed to provide large changes in control and response variables around nominal trim points. The technique of state estimation was used to combine radar tracking measurements and on-board inertial and air data measurements to obtain the best estimates of the aircraft kinematic variables. The state-estimation procedure produced a consistent data set that includes estimates of the unmeasured angular accelerations and flightpath winds. The availability of an engine model made it possible to isolate engine effects and determine aerodynamic forces and moments.

The completed VSRA data base consists of the set of individual 3-5-min flight-test maneuvers that covers the required flight envelope. The nominal trim points used to generate the data base have been presented along with data from representative flight-test maneuvers. A typical V/STOL maneuver from the data base has been used to illustrate the state-estimation procedure and the methods used to isolate the aerodynamic forces and moments. Long (15-30-min) records, consisting of concatenated time segments from several maneuvers, can be created and used to identify parameters in each model section. Work on developing the VSRA aerodynamic model from the data base is now in progress.

## Acknowledgment

The authors thank Miné Hagen, Vafa Kordestani, Suzi Kovacevich, Tom Schultz, and Phil Smith for their contributions to the work reported in this paper.

## References

- <sup>1</sup>Anderson, L. C. and Bunnell, J. W., "AV-8B Simulation Model Engineering Specification (Version 2.2)," Systems Control Technology, Inc., Palo Alto, CA, Nov. 1985.
- <sup>2</sup>Klein, V. and Batterson, J. G., "Determination of Airplane Model Structure from Flight Data Using Splines and Stepwise Regression," NASA TP-2126, 1983.
- <sup>3</sup>Draper, N. R. and Smith, H., Applied Regression Analysis (Chap. 6), John Wiley and Sons, Inc., New York, 1981.
- <sup>4</sup>Klein, V. and Batterson, J. G., "Aerodynamic Parameters Estimated from Flight and Wind-Tunnel Data," AIAA Journal of Aircraft, Vol. 23, No. 4, Apr. 1986, pp. 306-312.

- <sup>5</sup>Anderson, L. C. and Hansen, R. S., "Review of AV-8B Aerodynamic Model Identification," Systems Control Technology, Palo Alto, CA, Oct. 1987.
- <sup>6</sup>Breeman, J. H., Erkelens, L. J. J., and Nieuwpoort, A. M. H., "Determination of Performance and Stability Characteristics from Dynamic Manoeuvres with a Transport Aircraft Using Parameter Identification Techniques," AGARD CP-373, 1984.
- <sup>7</sup>Bach, R. E., Jr. and Wingrove, R. C., "Applications of State Estimation in Aircraft Flight-Data Analysis," AIAA Journal of Aircraft, Vol. 22, No. 7, July 1985, pp. 547-554.
- <sup>8</sup>Stalford, H. L. and Ramachandran, S., "Application of the Estimation-Before-Modelling (EBM) System Identification Method to the High Angle-of-Attack/Sideslip Flight of T-2C Jet Trainer Aircraft," NADC-76097-30, June 1978.
- <sup>9</sup>Klein, V. and Schiess, J. R., "Compatibility Check of Measured Aircraft Responses Using Kinematic Equations and an Extended Kalman Filter," NASA TN D-8514, 1977.
- <sup>10</sup>Hansen, R. S., "DEKFIS User's Guide--Discrete Extended Kalman Filter/Smoothing Program for Aircraft and Rotorcraft Data Consistency," NASA CR-159081, 1979.
- <sup>11</sup>Sri-Jayantha, M. and Stengel, R. F., "Data Acquisition System and Methodology for High Angle of Attack Parameter Estimation," SAE Paper No. 830719, 1983.
- <sup>12</sup>McNally, B. D., "Full-Envelope Aerodynamic Modelling of the Harrier Aircraft," NASA TM-88376, 1986.
- <sup>13</sup>De Boor, C., "A Practical Guide to Splines," Applied Mathematical Sciences, Vol. 27, Springer-Verlag, Inc., New York, 1978.
- <sup>14</sup>Anderson, L. C., "AV-8B System Identification Results: Lateral-Directional Model, Ground Effects, and High Angle-of-Attack Model," Systems Control Technology, Inc., Palo Alto, CA, June 1986.
- <sup>15</sup>Gerlach, O. H., "Determination of Performance, Stability and Control Characteristics from Measurements in Nonsteady Maneuvers," AGARD CP-17, Pt. 1, 1966, pp. 499-523.
- <sup>16</sup>Wingrove, R. C., "Quasilinearization Technique for Estimating Aircraft States from Flight Data," AIAA Journal of Aircraft, Vol. 10, No. 5, May 1973, pp. 303-307.
- <sup>17</sup>Maine, R. E. and Iliff, K. W., "Application of Parameter Estimation to Aircraft Stability and Control--The Output-Error Approach," NASA RP-1168, 1986.
- <sup>18</sup>YAV-8B Simulation and Modelling, Vol. 1, Aircraft Description and Program Summary," NASA CR-170397, 1983.
- <sup>19</sup>Bach, R. E., Jr., "State Estimation Applications in Aircraft Flight-Data Analysis (A User's Guide for SMACK)," to be published, June 1988.
- <sup>20</sup>Bach, R. E., Jr., "Variational Algorithms for Nonlinear Smoothing Applications," NASA TM-73211, 1977.
- <sup>21</sup>Bach, R. E., Jr., "A Variational Technique for Smoothing Flight-Test and Accident Data," AIAA Journal of Aircraft, Vol. 19, no. 7, July 1982, pp. 546-552.
- <sup>22</sup>Bach, R. E., Jr. and McNally, B. D., "A Flight-Test Methodology for Identification of an Aerodynamic Model for a V/STOL Aircraft," NASA TM-100067, 1988.
- <sup>23</sup>Franklin, J. A., "VSRA Air Data Calibration," Internal Memorandum, NASA Ames, Oct. 1987.
- <sup>24</sup>"Pegasus Engine 8735 Bleed Flow Calibration at Patuxent River," Rolls-Royce Inc., Atlanta, GA, ATR 0703, Dec. 1987.

Table 1 Variable list for aerodynamic model data base

Variable	Measured	Estimated
Euler angles	Onboard	SMACK
Angular rates	Onboard	SMACK
Angular accelerations		SMACK
Linear accelerations	Onboard	SMACK
Positions relative to Earth	Radar	SMACK
Velocities relative to Earth		SMACK
Airflow angles	Onboard	SMACK
Static pressure	Onboard	
Total pressure	Onboard	SMACK
Total temperature	Onboard	
True airspeed		SMACK
Flightpath winds		SMACK
Flap setting	Onboard	
Aileron deflections	Onboard	
Stabilator deflection	Onboard	
Rudder deflection	Onboard	
Engine nozzle angle	Onboard	
Engine fan speed	Onboard	
Compressor pressure	Onboard	
Fuel and water weights	Onboard	
RCS roll-valve positions	Onboard	
RCS pitch-valve positions	Onboard	
RCS yaw-valve position	Onboard	
Engine and RCS body forces		ENCAL
Engine and RCS moments		ENCAL
Gross weight and inertias		ENCAL

Note: SMACK is the state estimation program; ENCAL is the propulsion model of the VSRA engine.

Table 2 Nominal trim conditions for jet velocity ratio-angle of attack maneuver

Nozzle, deg	Flap, deg	AOA, deg
2 (full-aft)	5	5
		10
	25 (STOL) <sup>a</sup>	15
		5
10	25 (STOL)	5
		10
		15
30	5	5
		10
		15
	35 (STOL)	5
		10
45	54 (STOL)	5
		10
		15
60	61 (STOL)	5
		10

<sup>a</sup>VSRA STOL flap mode engaged; flaps scheduled as function of nozzle angle.<sup>18</sup>

Table 3 Nominal trim conditions for longitudinal and lateral maneuvers

Nozzle, deg	Flap, deg	Speed	AOA, deg	Maneuver(s)	
2 (full-aft)	5	0.3 M	--	1 Long., 1 lat.	
		0.4 M	--	1 Long.	
		0.5 M	--	1 Long., 1 lat.	
		0.7 M	--	2 Long., 2 lat.	
		--	12	1 Long. <sup>a</sup>	
	15	0.3 M	--	1 Long., 1 lat.	
		0.5 M	--	1 Long., 1 lat.	
	25	25	0.3 M	--	1 Long., 1 lat.
			--	12	1 Long. <sup>a</sup>
			--	--	--
25	5	--	10	1 Long., 1 lat.	
		--	2.5	1 Long. <sup>a</sup>	
		--	7	1 Long. <sup>a</sup>	
		--	13	1 Long. <sup>a</sup>	
	15	--	10	1 Long.	
		25	0.3 M	--	1 Long., 1 lat.
	--		0.5	1 Long. <sup>a</sup>	
	--		13	1 Long. <sup>a</sup>	
	--		--	--	
	40	5	--	9	1 Long. <sup>a</sup>
--			12	1 Long. <sup>a</sup>	
15		--	6	1 Long.	
		25	--	10	1 Long., 1 lat.
--			12	1 Long. <sup>a</sup>	
48 (STOL) <sup>b</sup>		130 KIAS	--	1 Long., 2 lat.	
60	61 (STOL)	--	10	1 Long., 1 lat.	
		--	12	1 Long. <sup>a</sup>	

<sup>a</sup>ASAS on.

<sup>b</sup>VSRA STOL flap mode engaged; flaps scheduled as function of nozzle angle.<sup>18</sup>

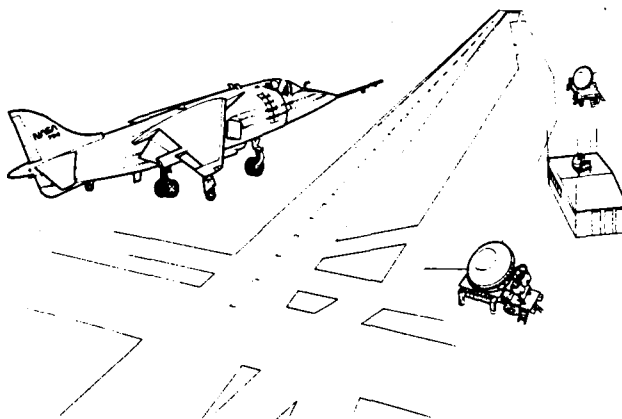


Fig. 1 V/STOL Research Aircraft and NASA facility at Crows Landing, California.

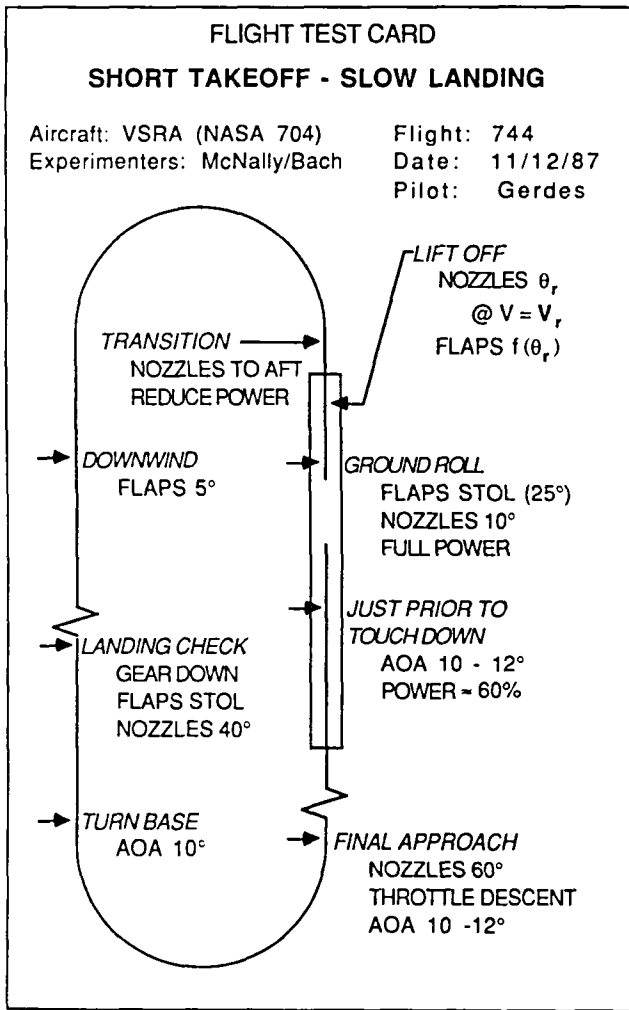


Fig. 2 Flight-test card for short-takeoff and slow landing maneuver.

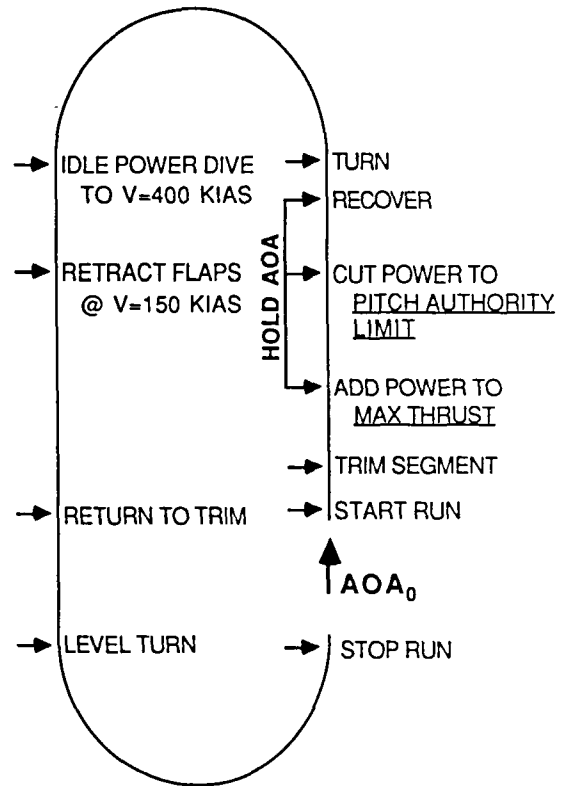


Fig. 3 Description of jet velocity ratio-angle of attack maneuver for flight-test card.

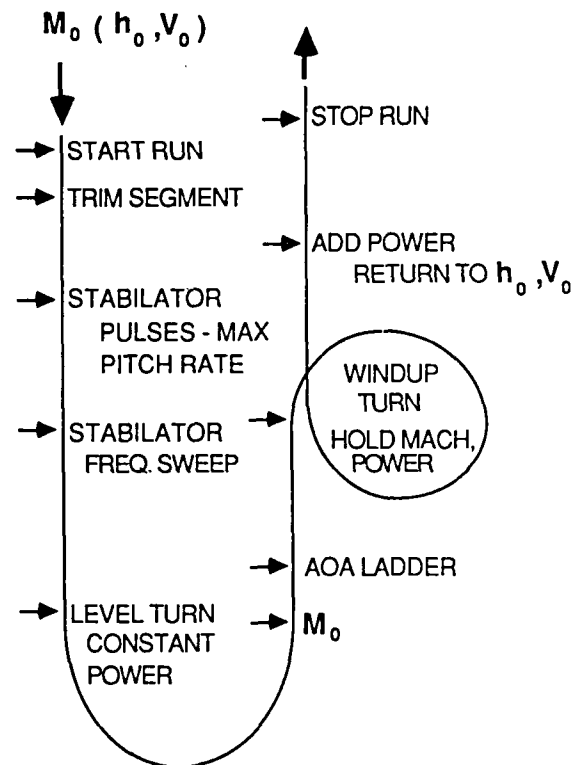


Fig. 4 Description of longitudinal maneuver for flight-test card.

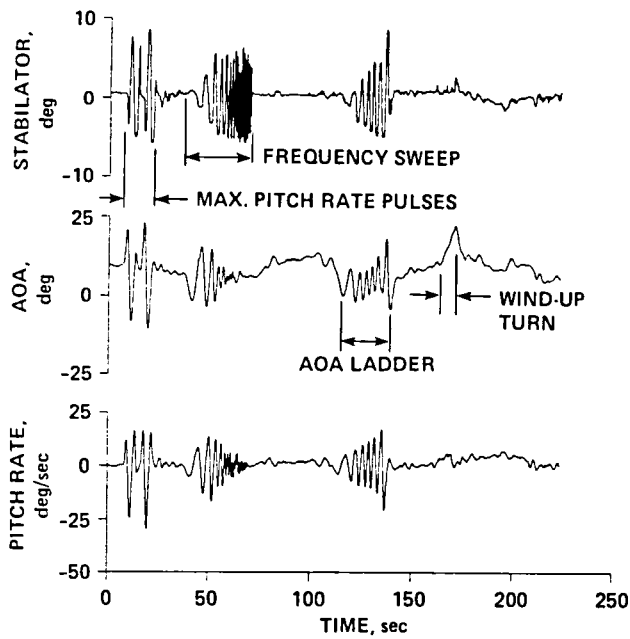


Fig. 5 Variation in stabilator, angle of attack, and pitch rate, during longitudinal maneuver: nozzles 60°, flaps 60°,  $V_0 = 85$  KIAS, and  $h_0 = 10,000$  ft.

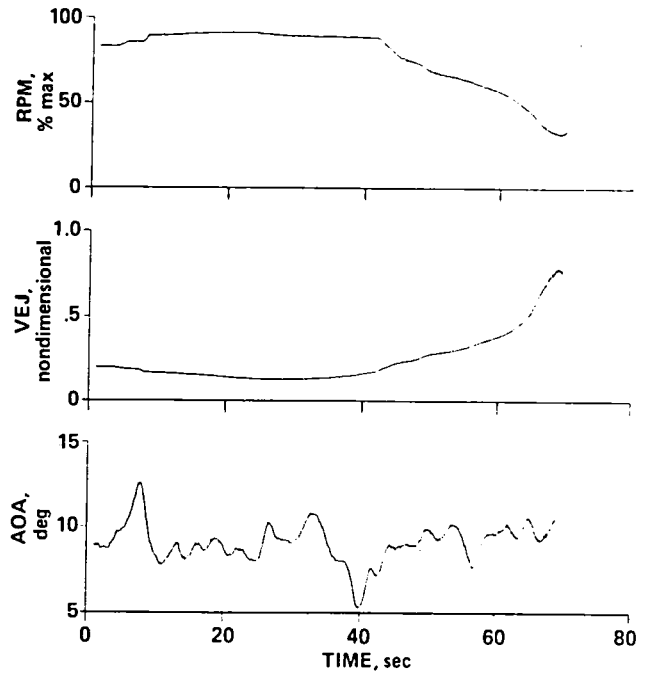


Fig. 7 Variation in engine rpm, jet velocity ratio, and angle of attack during first segment of jet velocity ratio angle of attack maneuver: nozzles 60°, flaps 60°, AOA = 10°,  $h_0 = 7,000$  ft.

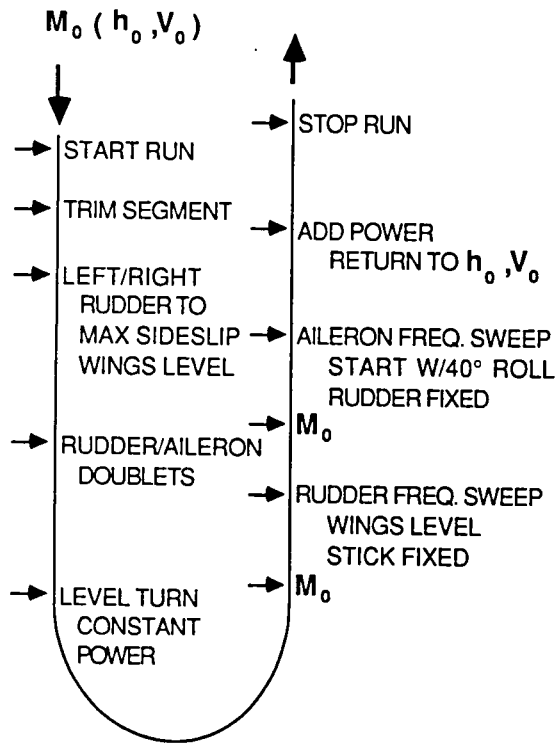


Fig. 6 Description of lateral maneuver for flight-test card.

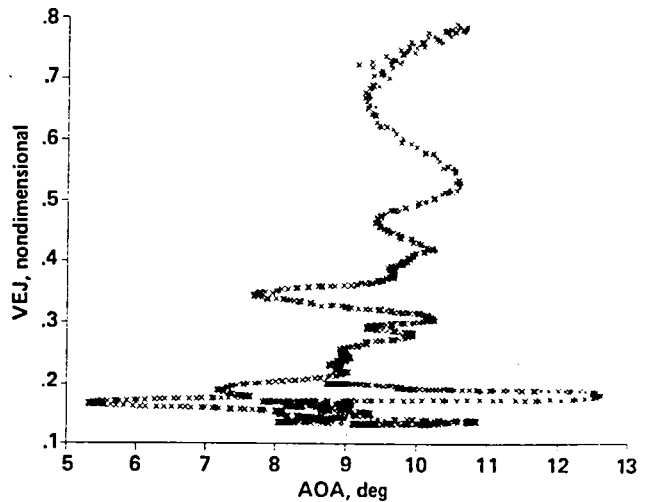


Fig. 8 Cross-plot showing jet velocity ratio versus angle of attack during first segment of jet velocity ratio angle of attack maneuver.

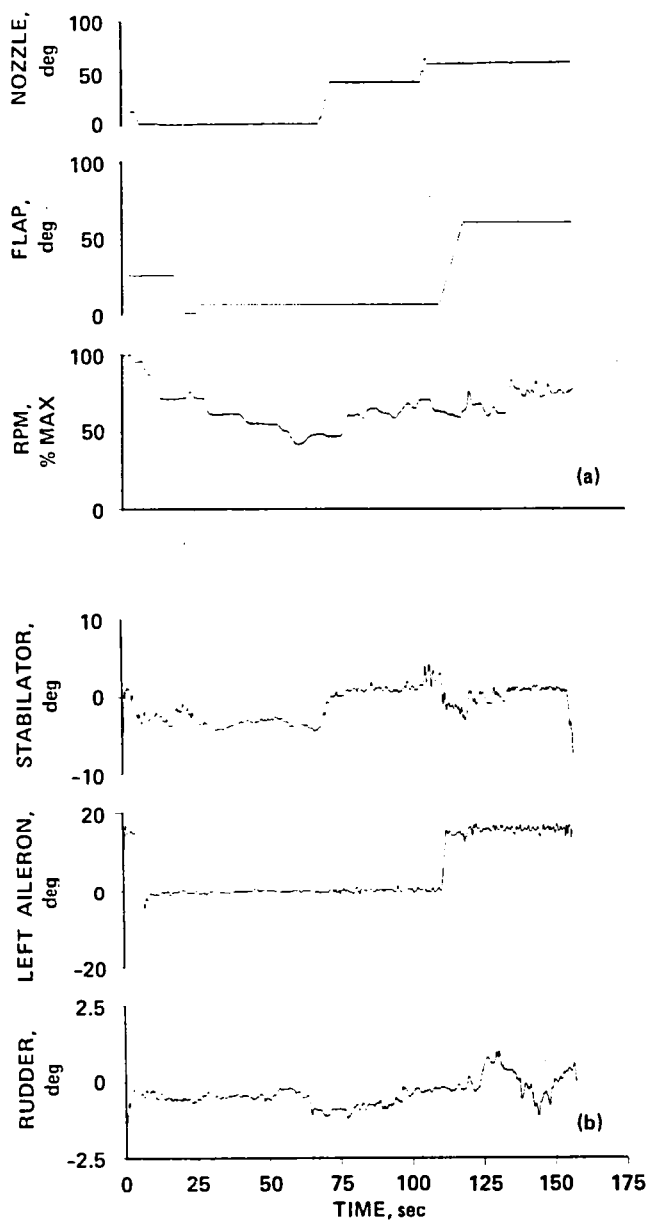


Fig. 9 Variation in nozzle angle, flap deflection, engine rpm, and control-surface positions during short-takeoff and slow-landing maneuver.

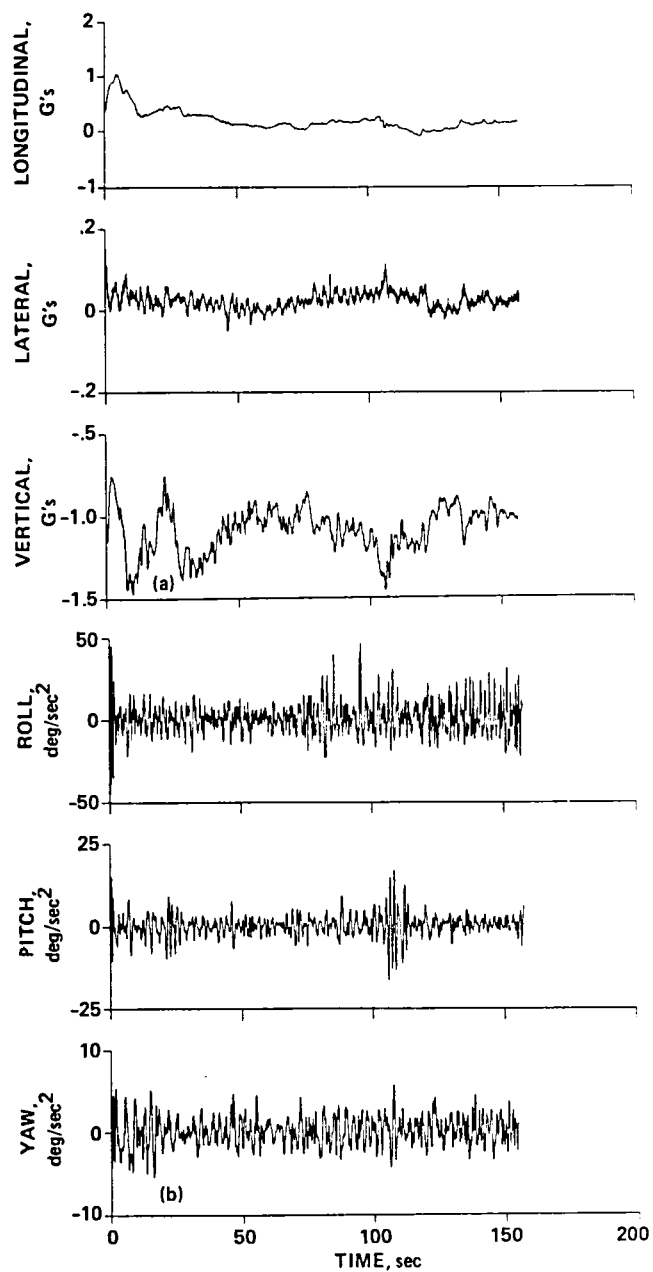


Fig. 10 Estimates of accelerations for short-takeoff and slow-landing maneuver. a) Linear accelerations. b) Angular accelerations.



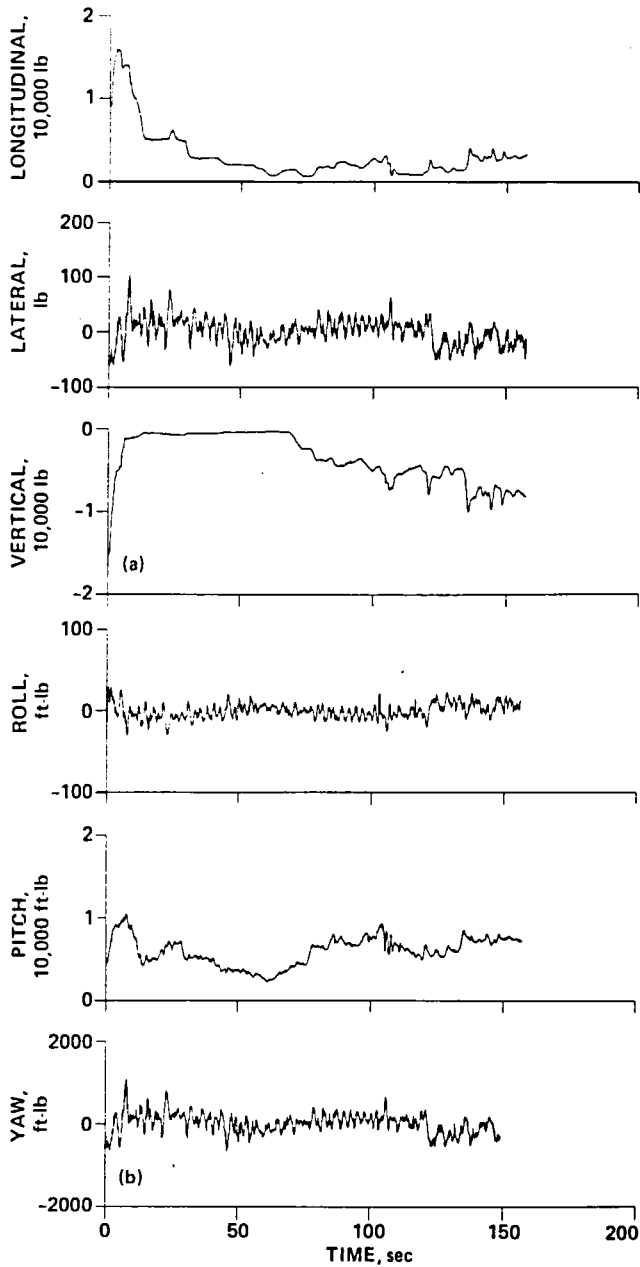


Fig. 11 Body-axis forces and moments due to engine and reaction control system thrust for short-takeoff and slow-landing maneuver. a) Forces. b) Moments.

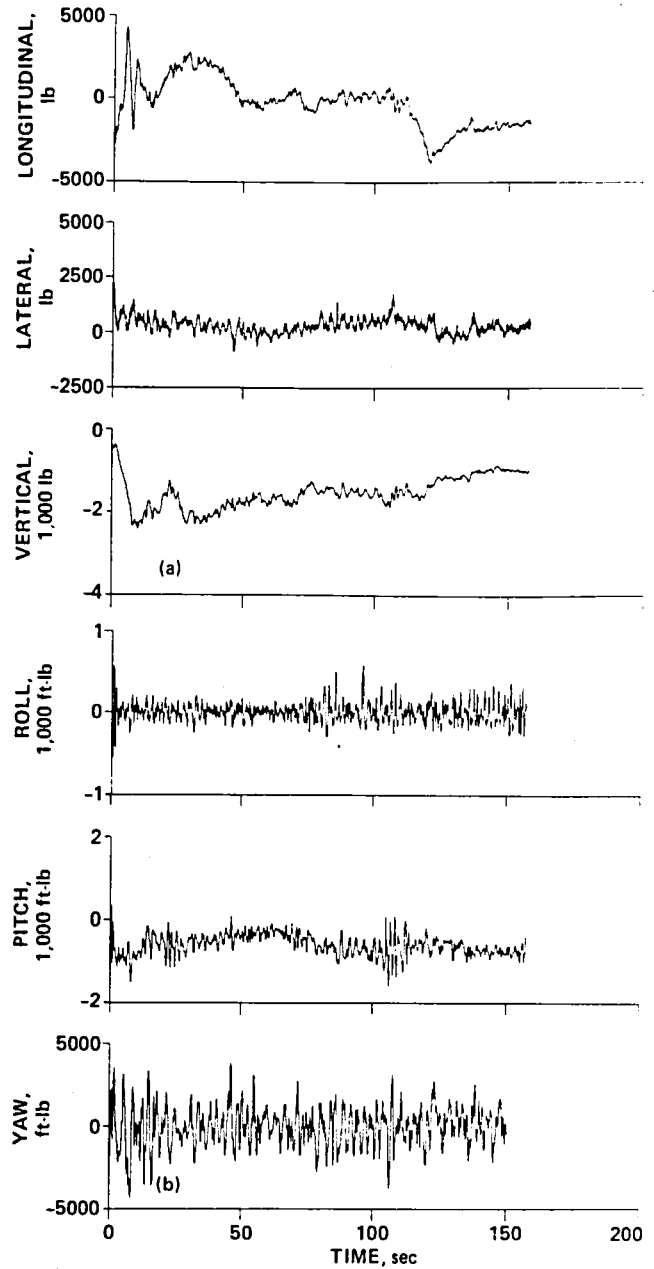


Fig. 12 Body-axis forces and moments due to aerodynamics for short-takeoff and slow-landing maneuver. a) Forces. b) Moments.

1. Report No. NASA TM-100996		2. Government Accession No.		3. Recipient's Catalog No.	
4. Title and Subtitle  Flight Testing a V/STOL Aircraft to Identify a Full-Envelope Aerodynamic Model				5. Report Date May 1988	
				6. Performing Organization Code	
7. Author(s)  B. David McNally and Ralph E. Bach, Jr.				8. Performing Organization Report No. A-88139	
				10. Work Unit No. 505-66-41	
9. Performing Organization Name and Address  Ames Research Center Moffett Field, CA 94035				11. Contract or Grant No.	
				13. Type of Report and Period Covered Technical Memorandum	
12. Sponsoring Agency Name and Address  National Aeronautics and Space Administration Washington, DC 20546-0001				14. Sponsoring Agency Code	
15. Supplementary Notes  Point of Contact: B. David McNally, Ames Research Center, MS 210-9 Moffett Field, CA 94035 (415) 694-5440 or FTS 464-5440					
16. Abstract  Flight-test techniques are being used to generate a data base for identification of a full-envelope aerodynamic model of a V/STOL fighter aircraft, the YAV-8B Harrier. The flight envelope to be modeled includes hover, transition to conventional flight and back to hover, STOL operation, and normal cruise. Standard V/STOL procedures such as vertical takeoff and landings, and short takeoff and landings are used to gather data in the powered-lift flight regime. Long (3-5 min) maneuvers which include a variety of input types are used to obtain large-amplitude control and response excitations. The aircraft is under continuous radar tracking; a laser tracker is used for V/STOL operations near the ground. Tracking data are used with state-estimation techniques to check data consistency and to derive unmeasured variables, for example, angular accelerations. A propulsion model of the YAV-8B's engine and reaction control system is used to isolate aerodynamic forces and moments for model identification. Representative V/STOL flight data are presented. The processing of a typical short-takeoff and slow-landing maneuver is illustrated.					
17. Key Words (Suggested by Author(s)) Flight testing Data consistency analysis Aerodynamic modeling V/STOL aircraft YAV-8B			18. Distribution Statement Unclassified-Unlimited  Subject Category - 05		
19. Security Classif. (of this report) Unclassified		20. Security Classif. (of this page) Unclassified		21. No. of pages 15	22. Price A02